Does global warming cause more extreme seasonal-to-interannual precipitation anomalies in Southwestern North America?

Laura Vogel (Columbia College)
Adviser: Richard Seager (Lamont-Doherty Earth Observatory)

Introduction

A popular idea surrounding the subject of climate change is that greenhouse warming will lead to 'more severe and frequent' droughts. IPCC multi-model ensemble means have already projected a shift to a drier climate beginning in the late 20th century to the early 21st century in southwestern North America (Seager et al. 2007). This is a regional effect of the poleward expansion of the subtropical dry zone and intensified water vapor transports from rising humidity, causing wet and dry climates to become more extreme (Held and Soden 2006). The drying of southwestern North America (SWNA) is clear and robust in projections of changes in precipitation – evaporation (P-E) anomalies averaged over time periods of more than a decade or so. However, this shift will not necessarily lead to increased variability or more extreme seasonal-to-interannual (S/I) departures from the new base state. Our objective was to determine whether models project 'more severe and frequent droughts' in the sense of larger S/I precipitation variability in SWNA. Tropical Pacific sea surface temperature (SST) variability drives much of the S/I precipitation in SWNA so we also study changes in the relationship between P-E and SST.

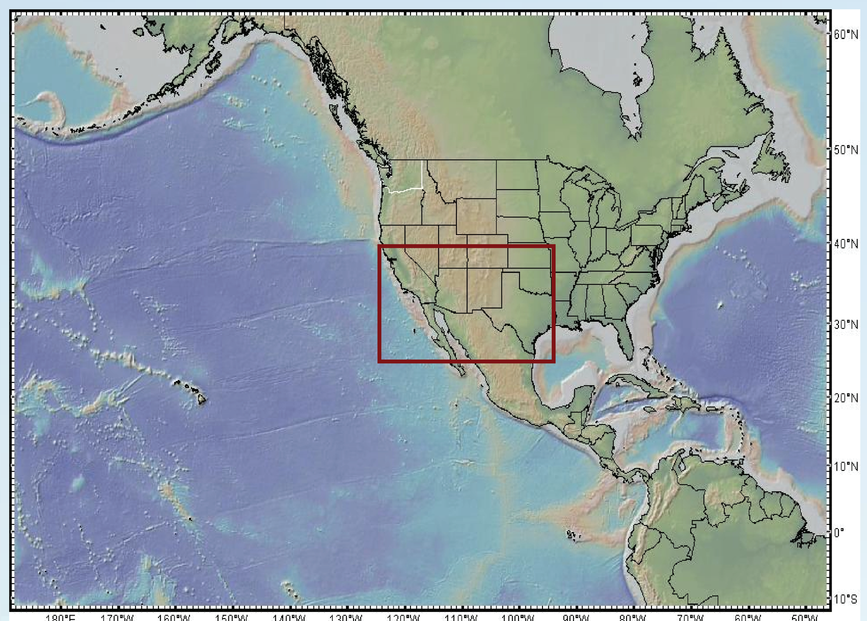

Southwestern North America: 25-40N, (125W)-(95W)

Data and Methods

We used data from all the 24 IPCC global climate models used in the Fourth Assessment Report, following the A1B emission scenario which assumes that CO_2 emissions increase until the year 2050 and decrease afterwards to 720ppb in 2100. Histograms of summer and winter precipitation and P-E anomalies were created for each model and cumulatively. An increase in variability would appear as a wider distribution in histograms of projected 21st century precipitation and P-E anomalies relative to the distribution of the 20th century anomalies.

A linear regression was also used between the tropical Pacific SST index and three variables: P-E, geopotential height, and zonal wind anomalies. The SST index is computed as surface temperature anomalies over the tropical Pacific region (5S-5N, 180W-90W), where SST variability is dominated by the El Niño Southern Oscillation. The SWNA region of precipitation is defined as land areas 25-40N and 125W-95W. Two regions of geopotential height were correlated and regressed with SSTs in the tropical Pacific, the area immediately above and the Aleutian Low region above the Northern Pacific Ocean. Height anomalies in these regions impact the jet stream which steers storm systems into western North America.

Observed data for the three variables and SSTs was also used to provide a standard for the models' 20th century projections; precipitation from the Global Precipitation Climatology Center, SSTs from the Hadley Center (both from 1901-2007), and height and zonal wind from NCEP/NCAR Reanalysis (1949-2010). Detrending was applied to remove the drying or warming changes in the mean climate from the time series, so that the direct relationship between P-E, SST, height, and wind variability could be isolated. These results are presented as bar graphs and maps, allowing side-by-side comparison of the 20th and 21st century correlation and regression coefficients.

Results

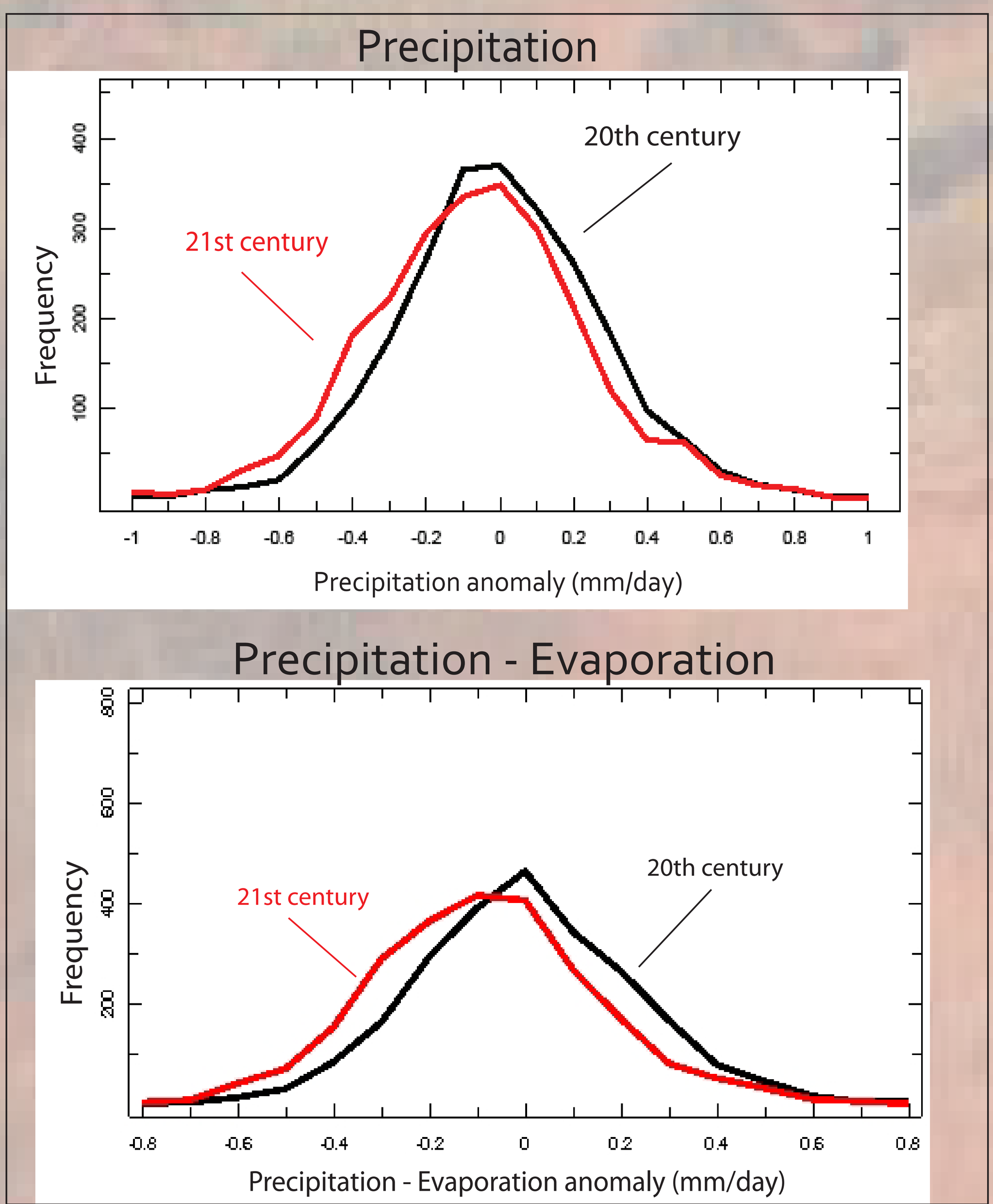

Figure 1: histogram of precipitation anomalies from all models (top), and histogram of P-E anomalies (bottom) for the winter season (October-March). P-E in SWNA region: 25-40N and 125W-95W. Anomalies relative to the 20th century climatology.

Precipitation - Evaporation and SST anomalies

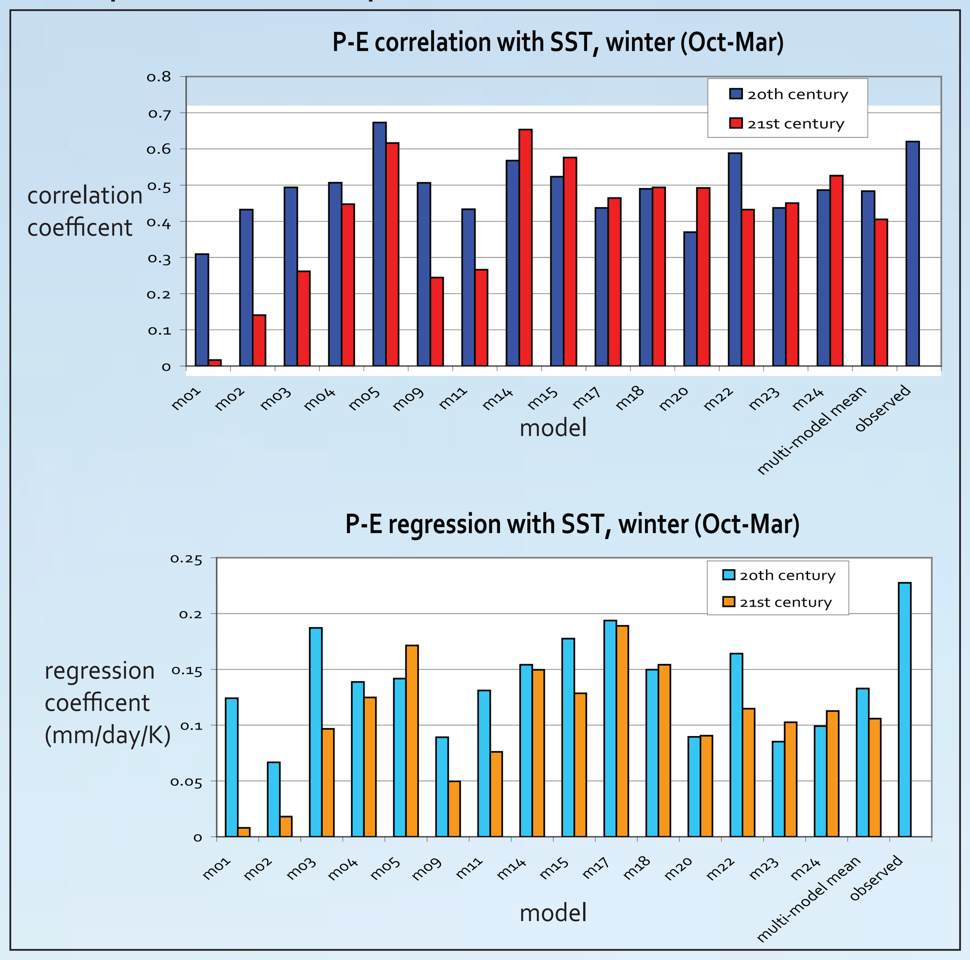

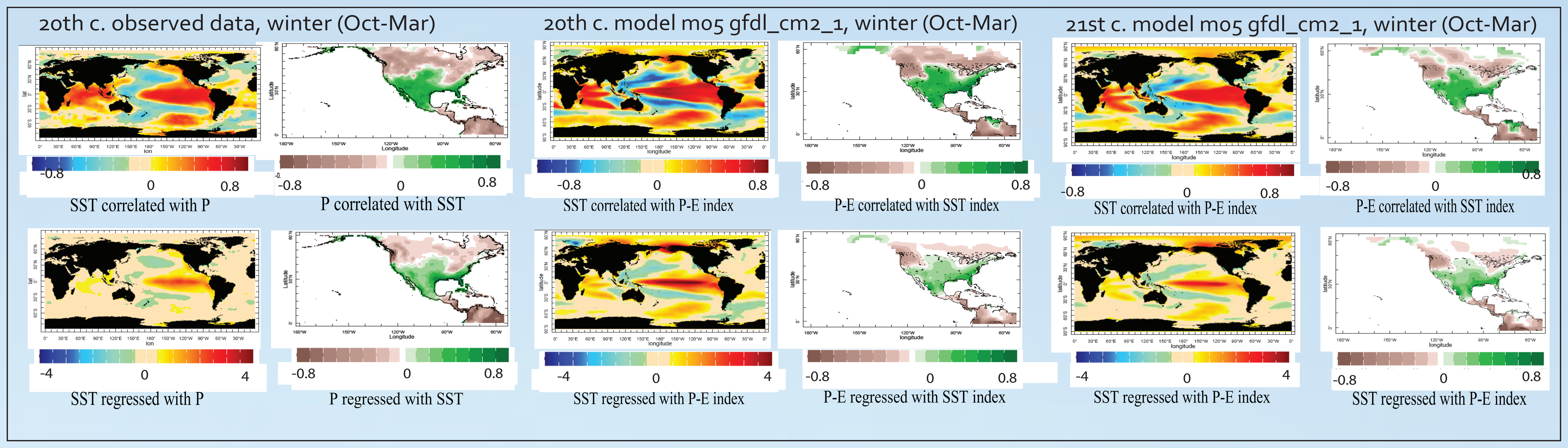

Figure 2 (left): bar graphs of correlation coefficients (top) and regression coefficients (bottom) for P-E and tropical Pacific SSTs. P-E in SWNA region: 25-40N and 125W-95W, tropical Pacific SSTs: 5S-5N and 180E-90W. Anomalies relative to the climatology of that century (1900-1999 or 2000-2099). 15 out of 24 models used; those with the closest correlation to observed (above 0.3). Also shown, the 15-model mean.

Figure 3 (above): P-E and SST index correlation and regression maps for 20th c. observed data and 20th and 21st c. simulations. Model mo5 GFDL CM2.1 created by the Geophysical Fluid Dynamics Laboratory of NOAA was chosen as a reasonable approximation of observed patterns and strengths.

Geopotential height and SST anomalies

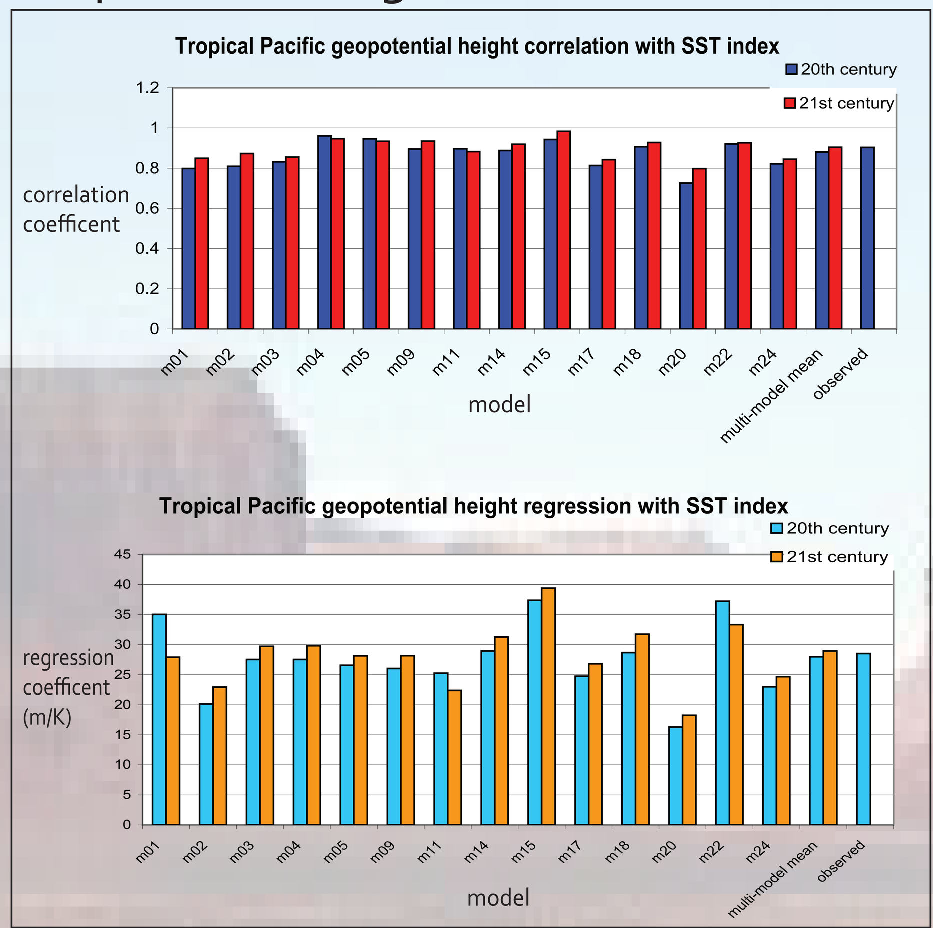

Figure 4 (above): bar graph of correlation coefficients (top) and regression coefficients (bottom) for 200 mbar geopotential height in the tropical Pacific and SSTs, using the same models excluding m23 which did not have the required data. Geopotential height region: 10S-10N and 150E-90W, tropical Pacific SSTs: 5S-5N and 180E-90W.

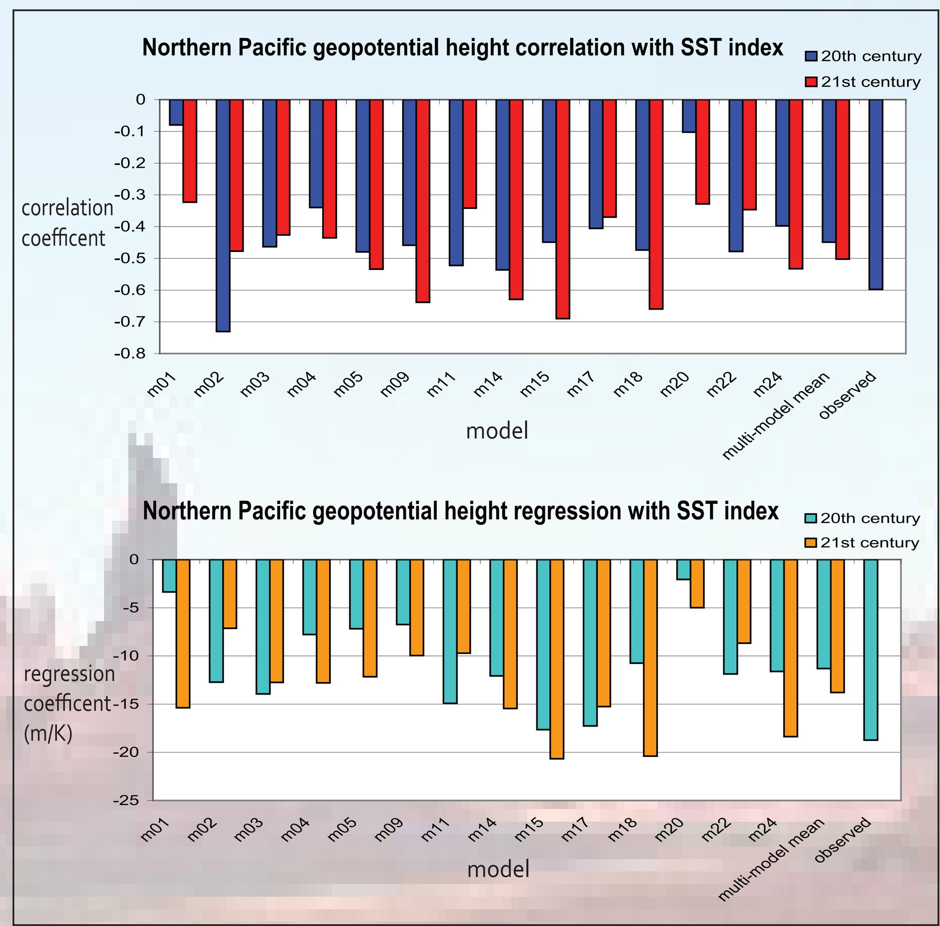

Figure 5 (above): bar graphs of correlation coefficients (top) and regression coefficients (bottom) for 200 mbar geopotential height in the northern Pacific and SSTs. This region has a negative correlation and regression with tropical Pacific SSTs. Geopotential height region: 30-60N and 170E-120W, tropical Pacific SSTs: 5S-5N and 180E-90W.

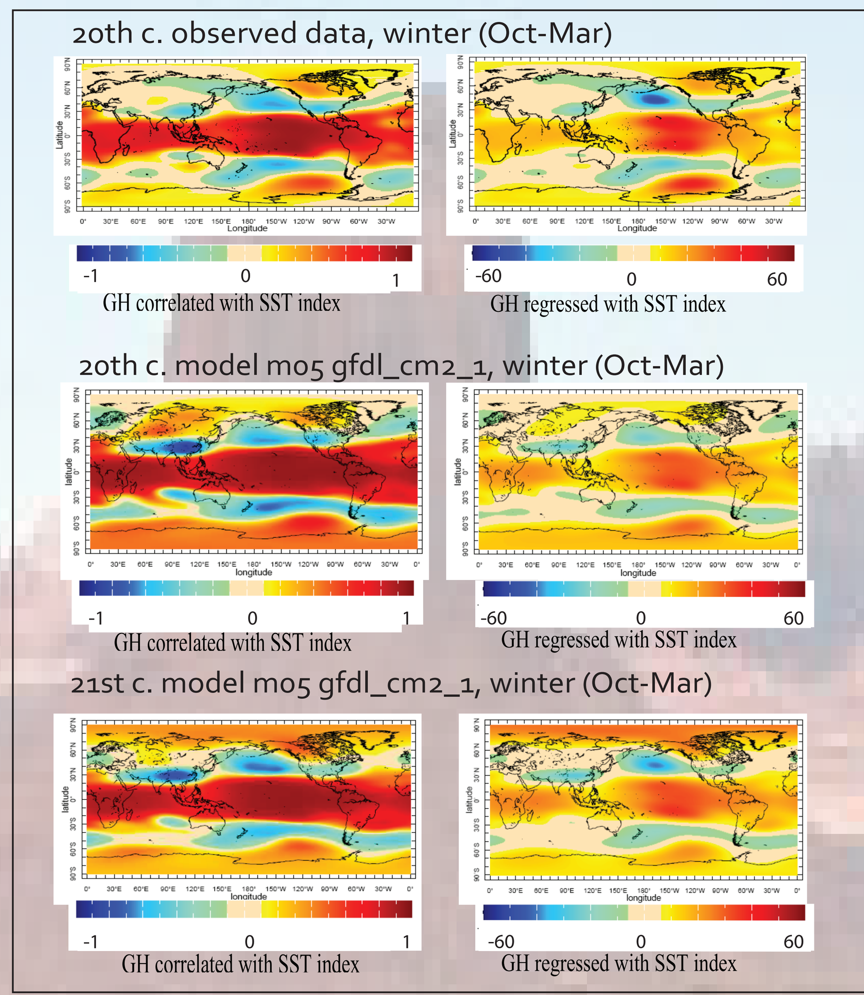

Figure 6: 200 mbar geopotential height and SSTs correlation and regression maps for 20th c. observed data and 20th and 21st c. simulations from model GFDL CM2.1.

Zonal wind and SST anomalies

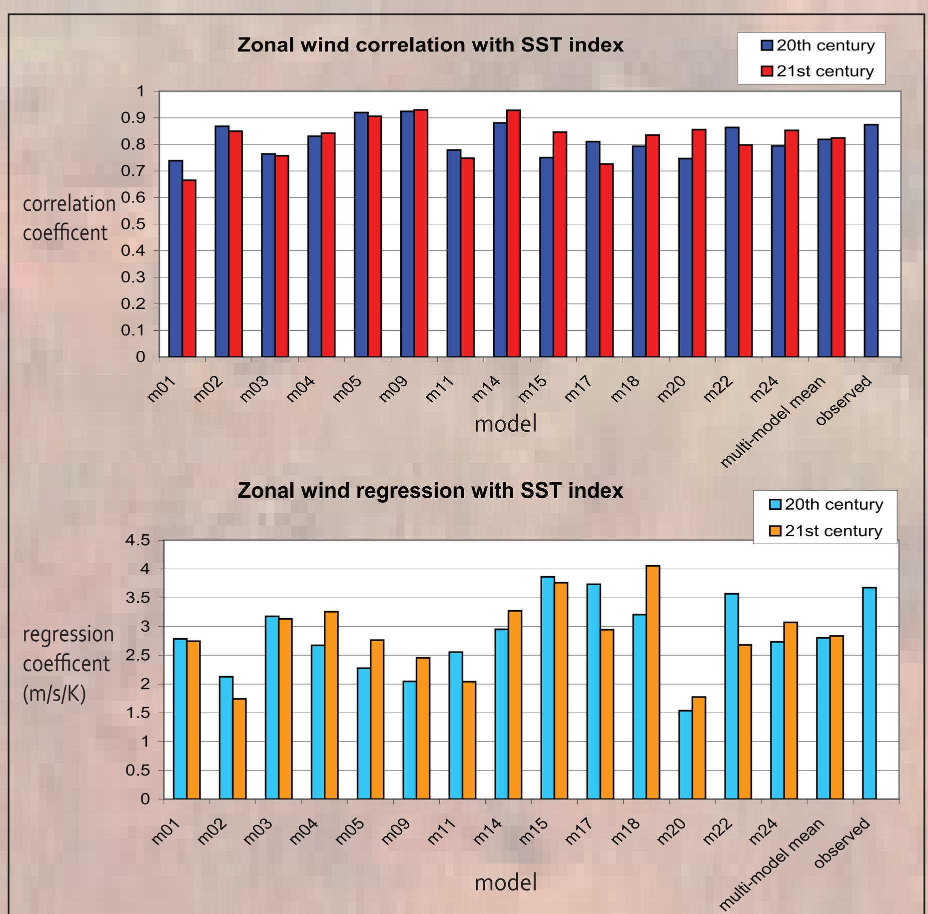

Figure 7: bar graph of correlation coefficients (top) and regression coefficients (bottom) for 200 mbar zonal wind and SSTs, using the same models for geopotential height. Zonal wind region: 20-40N and 170E-120W, tropical Pacific SSTs: 5S-5N and 180E-90W.

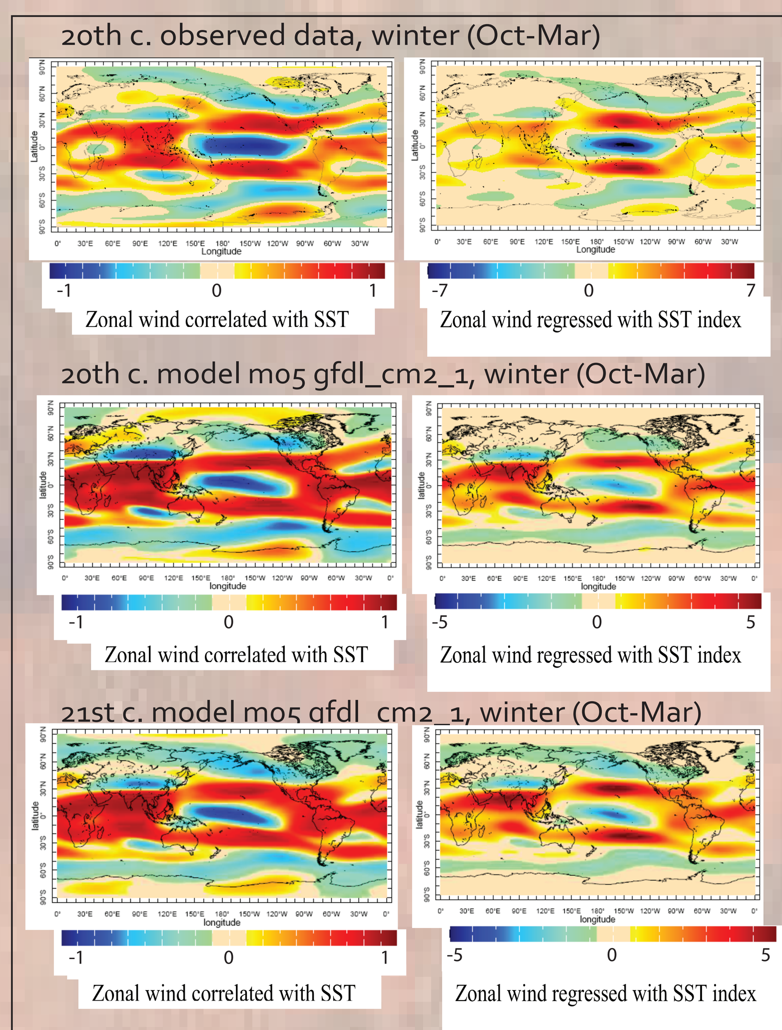

Figure 8: Zonal wind and SSTs correlation and regression maps for 20th c. observed data and 20th and 21st c. simulations from model GFDL CM2.1.

Results Continued

The histograms for 21st century precipitation and P-E in Figure 1 do not noticeably widen compared to the 20th century distributions, showing that S/I variability does not seem to increase due to warming. Because anomalies are computed relative to the 20th century mean, the peak shifts left showing the mean drying. The focus is on winter because it is the moisture supply season and drives summer conditions.

The 15-model mean correlation and regression coefficients of P-E with the SST index, shown in Figure 2, actually decrease slightly in the 21st century, indicating that a given SST anomaly would cause weaker P-E anomalies. Figure 3 shows the GFDL CM2.1 model's fairly close approximation to observed data with warm tropical Pacific SSTs forcing precipitation in SWNA. The GFDL CM2.1 model is typical in that the relationship weakens in the 21st century but retains the same spatial pattern. Summer was confirmed to have a weaker correlation with SSTs and is again not the focus. In contrast to the relations between P-E and SST, the correlation and amplitude of geopotential height anomalies with tropical Pacific SST anomalies strengthen (Figures 4 and 5). This increase in the amplitude of height anomalies does not, however, translate into an increase in the amplitude of zonal wind anomalies over the North Pacific, because mean zonal wind correlation and regression do not change in the 21st century (Figure 7).

Conclusions

Although a given circulation anomaly operating on an atmosphere holding more moisture due to warming could cause larger amplitude P-E anomalies, this does not appear to be the case as seen by the distribution in the histograms and the correlation and regression between P-E and the SST index. The geopotential height anomalies over both the tropical and North Pacific do reach a larger amplitude and stronger correlation with the SST anomalies in the 21st century. This might be expected because of the possible increase of heating anomalies for a given SST anomaly, due to the nonlinear increase in specific humidity with temperature. However, geopotential height anomalies may not translate into an increase in the amplitude of zonal wind anomalies because other terms in the meridional momentum budget may change given that circulation is not in pure geostrophic balance. It is well-known that storm tracks change under global warming and will impact the mean winds. The mean zonal wind anomalies are important in 'steering' storm systems and determining where in western North America they bring precipitation (Seager et al. 2010). The fact that zonal wind anomalies over the North Pacific do not strengthen in response to global warming could explain why P-E variability does not increase even as geopotential height variability does. In future work we will further explore the behavior of P-E in SWNA in the 21st century's warming atmosphere and look at the dominant terms in the P-E balance to see which change. This will allow clarification of why the P-E amplitude relative to the SST index actually weakens even as humidity increases.

References:

Held, I.M. and B.J. Soden. Robust responses of the hydrological cycle to global warming. *J. Climate* 2006, *Volume 19*, 5686-5699.

Seager, R. et al. Model projections of an imminent transition to a more arid climate in southwestern North America. *Science* 2007, *Volume 316*, 1181-1184.

Seager, R. et al. Adjustment of the atmospheric circulation to tropical Pacific SST anomalies: Variability of transient eddy propagation in the Pacific-North America Sector. *Q. J. Roy. Meteor. Soc.* 2010, *Volume 136*, 277-296.

Acknowledgments: Thanks to Jenny Nakamura and Naomi Naik

Background: Photograph of Utah from tripadviser.com